Thermodynamic Balance of Three-Dimensional Stratospheric Winds Derived from a Data Assimilation Procedure

CLARK J. WEAVER

Applied Research Corporation, Landover, Maryland

ANNE R. DOUGLASS AND RICHARD B. ROOD

NASA/Goddard Space Flight Center, Greenbelt, Maryland

(Manuscript received 8 July 1992, in final form 4 February 1993)

ABSTRACT

The NASA/Goddard three-dimensional chemistry and transport model is driven by winds from a stratospheric data assimilation system. Synoptic- and planetary-scale patterns, apparent in satellite observations of trace constituents, are successfully reproduced for seasonal integrations. As model integrations proceed, however, the quality of simulations decreases, and systematic differences between calculation and measurement appear. The differences are explained by examining the zonal-mean residual circulation. The vertical residual velocity $\bar{w}^*$ is calculated two ways: (i) from the diabatic heating rates and temperature tendency and (ii) from the Eulerian vertical velocity and the horizontal eddy heat flux convergence. The results from these calculations differ substantially. Periodic insertion of observational data during the assimilation process continually shocks the general circulation model and produces these differences, which leads to an overestimate of the mean vertical heat and constituent transport. Such differences are expected to be general to all data assimilation products. This interpretation is corroborated by two-dimensional (2D) model calculations. When $\bar{w}^*$ is calculated from (ii), the 2D ozone evolution is unrealistic and qualitatively similar to the 3D model simulation. The 2D ozone evolution is reasonable when $\bar{w}^*$ is calculated from (i).

1. Introduction

The NASA/Goddard three-dimensional chemistry and transport model (CTM), which uses winds from a stratospheric data assimilation system, has been used to calculate the evolution of constituents such as nitric acid and ozone (Rood et al. 1989, 1991, 1992). Comparisons of calculated ozone and nitric acid values with measurements indicate that the assimilation performs well in representing the dynamics of synoptic and planetary waves. Many of the wintertime planetary- and synoptic-scale patterns apparent in satellite constituent observations are reproduced by model calculations. Furthermore, during individual events such as stratospheric warmings, the zonal-mean changes in the model are in good agreement with data. From the similarity of these aspects of the evolution of observed and simulated fields, we infer that the underlying mechanisms of the quasi-horizontal wave transport are accurately represented in the CTM.

The simulations described above have spanned only a few months. Even for these seasonal integrations, the calculated ozone fields become systematically low in the tropics when compared with Total Ozone Mapping Spectrometer (TOMS) and Limb Infrared Monitor of the Stratosphere (LIMS) measurements (Rood et al. 1991; Allen et al. 1991). For short calculations, the biases are not large enough to interfere with the model representation of planetary- and synoptic-scale events, but as the integration proceeds biases are found even at middle latitudes and the comparisons of data with the calculated fields are substantially degraded. It should be noted that because midlatitude ozone is long-lived in the lower stratosphere, with an equinoctial lifetime of 10 days at 10 hPa increasing to more than one year at 100 hPa, these differences do not result from the model photochemical representation.

The data assimilation system used to provide the winds for the transport is typical of systems used in numerical weather prediction. A general circulation model is used in conjunction with an objective analysis scheme. At six-hour intervals, data are inserted into the model using optimal interpolation analysis (Baker et al. 1987). The insertion of data produces wind and temperature fields that are close to observations, but keeps the model from developing an internal consistency. Data assimilation systems have been developed to address time scales of hours to days, which are important to weather prediction. Physical processes on

Corresponding author address: Dr. Clark J. Weaver, Code 916, NASA/GSFC, Greenbelt, MD 20771.

time scales much longer than the forecast/analysis time period (six hours) are not necessarily well represented.

Systematic differences between calculated and measured constituent concentrations at tropical and middle latitudes suggest problems with the mean meridional mass motions produced by the assimilation. It is much more difficult to assure that the mean meridional circulation from the assimilation is accurate than it is to simulate the behavior of the large-scale waves. In this paper the transformed Eulerian mean residual circulation will be used to examine the zonal-mean meridional constituent transport.

The residual circulation is largely driven by diabatic processes, and in two-dimensional models the residual and diabatic circulations have both been used to represent advective transport (WMO 1986; Geller et al. 1992). However, the residual circulation of the assimilated winds is often inconsistent with the diabatic heating term calculated in the assimilation. When the data are inserted there is no a priori reason to expect the correct balance to exist between the thermal fields and the velocity fields. Several important causes of this inconsistency can be identified. For instance, in the troposphere, where moisture data is assimilated, there is a spurious release of latent heat caused by imbalances between the moisture data, temperature, and the convective parameterization. In stratospheric general circulation models, the temperature field is usually colder than observations (Mahlman and Moxim 1987). Thus, in the assimilation procedure, insertion of observed temperatures must always counteract the model tendency toward a colder climatology.

More important for the current calculations is the fact that the thermal data and the horizontal wind fields are not balanced at the time of observation. Even where there are wind data from the sondes, the observational errors are large enough that the balance between the thermal field and wind field contains large errors. When there are no wind data, the most common case, the model and the analysis procedure must define the balance. However, unwanted inertial–gravity modes can be excited as a result of these observational errors and can affect the assimilated variables. These errors manifest themselves strongly in the residual vertical winds, causing the time-averaged circulation not to show the expected relationship to diabatic heating. This is a manifestation of the "spinup" problem, and is typical of all assimilation procedures (Daley 1991).

To be able to carry out longer simulations, it is necessary that the mean meridional mass motions produced by the assimilation reflect actual stratospheric transport. Our immediate interest is in producing accurate multiyear integrations to study the fate of supersonic aircraft exhaust. It is critical to determine the rate at which aircraft exhaust is dispersed horizontally and transported into the troposphere, where it is assumed to be removed rapidly through rainout processes. These processes determine the level of stratospheric pollutant expected after many years of fleet operations. Use of the transport model will allow determination of the fate of pollutants for different scenarios of flight operations for varying synoptic conditions, seasons, and years. Evaluation of the long-term behavior of aircraft exhaust is clearly sensitive to the mean meridional mass transport.

This study examines the biases found in the comparison of simulated ozone with TOMS and LIMS satellite measurements, and discusses the biases as they are related to the thermodynamic balance calculated from the assimilated wind fields. Further insight is gained by analyzing the two-dimensional (2D) residual circulation. The residual circulation is calculated from the heating rates and static stability (Dunkerton 1978) and from the dynamical definition as given by Andrews and McIntyre (1976, 1978) and Edmon et al. (1980). This approach allows interpretation of the transport processes in the three-dimensional (3D) model in terms of cross-isentropic (diabatic) transport and quasi-horizontal isentropic mixing as proposed by Mahlman (1985) and Holton (1986). Because the assimilated wind fields are known to be inaccurate at high southern latitudes, due primarily to analysis problems, this study will focus on the Northern Hemisphere.

2. Model description

The ozone simulations examined here use assimilated wind fields to drive the CTM. There is no feedback between the calculated ozone and the model winds, that is, the simulation is "off line" (Mahlman and Moxim 1978). The wind fields are taken from the stratospheric analysis system (STRATAN) described by Takano et al. (1987). The STRATAN winds are given at 4° latitude by 5° longitude; the vertical spacing is about 2 km in the troposphere and 3.5 km in the stratosphere. The winds are from the STRATAN 6-hour forecasts as described by Rood et al. (1991).

The selection and implementation of the numerical transport schemes in the CTM are described by Allen et al. (1991). The upstream monotonic scheme of van Leer (1974) is used for horizontal transport. This scheme has an inherent scale-dependent diffusion, which is countered somewhat by use of a higher horizontal resolution (2° lat by 2.5° long) than the wind fields. The vertical transport scheme conserves not only tracer mass but also the first and second moments of tracer distribution (Prather 1986). This scheme is nondiffusive, and is used for vertical transport in an effort to counter the coarse resolution and to maintain sharp mixing ratio gradients as for ozone at the tropopause. The justification and performance of this scheme is given by Rood et al. (1991, 1992).

The continuity equation is solved by process splitting; at each time step the advective contribution to the ozone change is calculated and then combined with the photochemical component. The production and

loss frequency are 15-day averages taken from the Goddard 2D model (Douglass et al. 1989). The simulation considered here is initialized on 1 December 1978; LIMS observations are used above 100 hPa and below this level the field is set to the zonal average from the 2D model. In the lower stratosphere, ozone is long-lived, with a lifetime greater than 50 days. For an integration of this duration, ozone may be considered a passive tracer.

3. Comparison with observations

A strong test of the assimilation dynamics is the degree to which constituent evolution calculated with the transport model matches observations. The comparison of measurements with calculated planetary- and synoptic-scale features is considered by Rood et al. (1991, 1992). Here we consider the global mass transport. To analyze the transport circulation of the CTM, the latitudinal slope of the zonal-mean ozone is compared with the slope of isentropes, as in Mahlman (1985). The slope of the modeled ozone isolines with respect to the isentropes is produced by competing processes. The residual circulation steepens the slope of the constituent with respect to isentropes, while quasi-horizontal isentropic mixing reduces this slope.

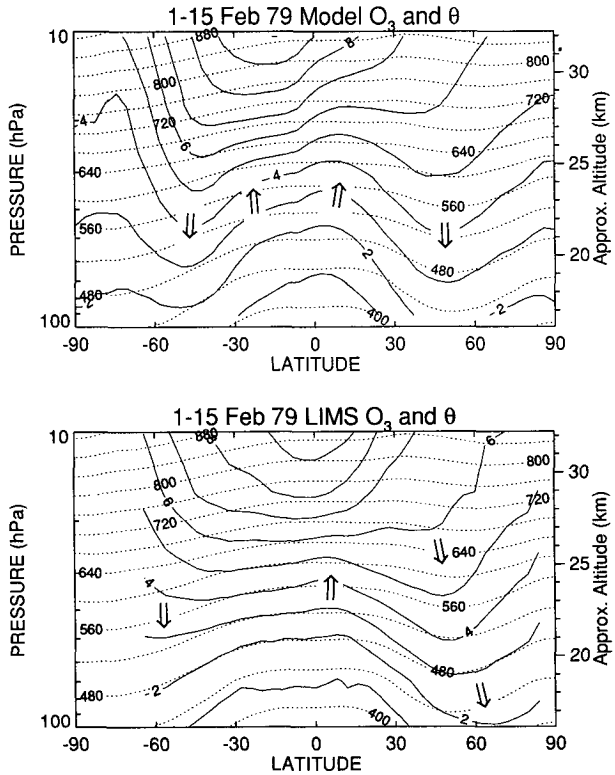

FIG. 1. (a) Zonal mean simulated ozone (ppm) from the 3D CTM and potential temperature and (b) zonal mean LIMS ozone (ppm) and potential temperature for 1–15 February 1979.

If the ozone isolines are parallel to the isentropes, then horizontal mixing dominates the transport. Conversely, if the ozone isolines are steep relative to the isentropes, the residual circulation is dominant.

a. Comparison with LIMS observations

The model calculation is initialized on 1 December 1978 using the LIMS data above 100 hPa, and for the first few days of integration the measured and simulated ozone contours relative to the isentropes are similar. However, the slope of the simulated ozone contours steepens rapidly during the first few weeks of the integration. Figure 1a shows the time average (1–15 February) of the model zonally averaged ozone as a function of latitude between 10 and 100 hPa. The 15-day average of the zonal average potential temperature is also given on this figure. At this time, two months into the integration, the ozone and theta surfaces are distinctly different, suggesting the strong role of the residual circulation.

The direction of the residual circulation may be inferred by examining the ridges and troughs in the ozone contours with respect to the isentropes, and is indicated in Fig. 1a by arrows. It is clear that there is strong downward motion at 50°S and 50°N with two upward branches in the tropics. Figure 1b shows the zonal-mean LIMS ozone averaged for the same period, and repeats the potential temperature as for Fig. 1a. The zonal-mean circulation inferred from observations has the same upward (downward) branches in the tropics (midlatitudes). However, the ozone contours are substantially less steep relative to the potential temperature contours, especially in the Southern Hemisphere. This suggests that the actual residual circulation is significantly less vigorous than the residual circulation of the assimilated data. Furthermore, the downward midlatitude branches at 100 hPa inferred from observations are poleward of the branches in the model calculation.

b. Comparison with TOMS measurements

A similar picture of the ozone transport in the simulation is found by comparing calculated total ozone with TOMS measurements. Figure 2 shows the time average (1–15 February) of the difference between the zonally averaged TOMS data and the global mean of the TOMS measurements and the difference between the zonally averaged model total ozone and the global mean of the model. The simulated total ozone exceeds TOMS data in the midlatitudes, where the excess downward transport is suggested by LIMS measurements. The latitudinal gradients of the calculated total ozone are much larger than the observed gradients in the subtropics and have steepened since the initialization. This is consistent with the excessive downward motion in the midlatitudes and excessive upward motion in the tropics.

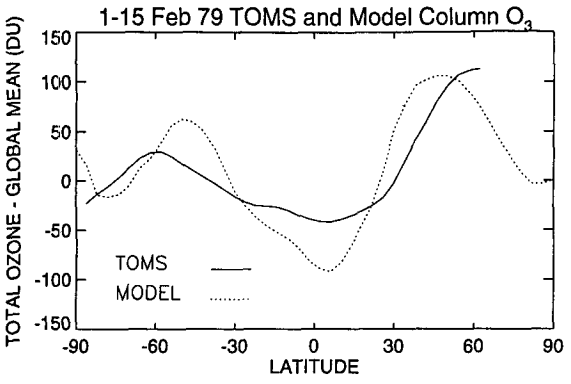

FIG. 2. Zonal mean total column ozone (Dobson units) from TOMS (solid) and 3D CTM (broken) for 1–15 February 1979.

This qualitative picture of the transport produced by the assimilation is also found in a 1989 ozone simulation. The calculated latitudinal ozone gradients are found to steepen noticeably relative to the observed gradients within the first few days of the simulation. These gradients steepen as the simulation continues (Allen et al. 1991), suggesting that the problems of excessive upward equatorial transport and excessive downward midlatitude transport are endemic to the assimilation procedure and not specific to 1979.

It is clear that the simulated ozone does not agree with measurements in important ways, suggesting that the actual stratospheric mass transport circulation must differ from that produced by the assimilated wind fields. Given the evidence that the quasi-horizontal wave transport is well represented, we infer that the residual circulation of the transport model is excessively strong upward in the tropics and downward at midlatitudes.

4. The thermodynamic balance of the assimilation

The zonal-mean thermodynamic equation is given by

$$\bar{w}\bar{\theta}_z + \frac{\bar{v}}{a}\bar{\theta}_\phi + \frac{1}{a\cos\phi}(\cos\phi\overline{v'\theta'})_\phi + \frac{1}{\rho}(\rho\overline{w'\theta'})_z + \bar{\theta}_t - \bar{Q} = 0; \quad (1)$$

w vertical velocity
v meridional velocity
θ potential temperature
z altitude
ϕ latitude
a radius of earth
ρ density
Q heating rate
( ) zonal average
′ deviation from the zonal average.

Subscripts denote derivative.

Except for the temperature tendency, these terms are evaluated using the STRATAN wind, temperature, and diabatic heating rate fields. STRATAN uses the radiative scheme of Rosenfield (1987) to calculate the diabatic heating rates.

Evaluation of the potential temperature tendency is problematic, because explicit values for time derivatives are not available. The difficulty is illustrated by examining the difference between analysis and forecast values of potential temperature. Figure 3 shows a time series of potential temperature (θ) at 53 hPa, 46°N, 0°E for seven successive 6-hour forecasts. Each forecast is represented by two connected solid line segments. The analysis values are indicated on the figure by A. Since they are used as the forecast initialization they may also be labeled 0F. The forecast values of θ at 3 and 6 hours after the initialization are indicated by 3F and 6F on the figure and connected by the solid line. The difference between θ at 6F from the forecast and θ at A from the analysis clearly demonstrates the shock to the model that occurs every 6 hours during the data insertion.

The time tendency of θ derived from the analysis for each 6-hour period is given by the slope of the dotted-line segment. The direction of the model (the prognostic tendency) is approximated by the slope of the solid line that connects forecast values 0F, 3F, and 6F. The slope of the dotted line is often sharply different than the slope of the concurrent solid line. This demonstrates that the prognostic tendency within the model and tendency derived from a time series of temperatures can differ. For this work, the temperature tendency is calculated from successive 6-hour forecast fields since the forecast fields are used in the ozone transport model.

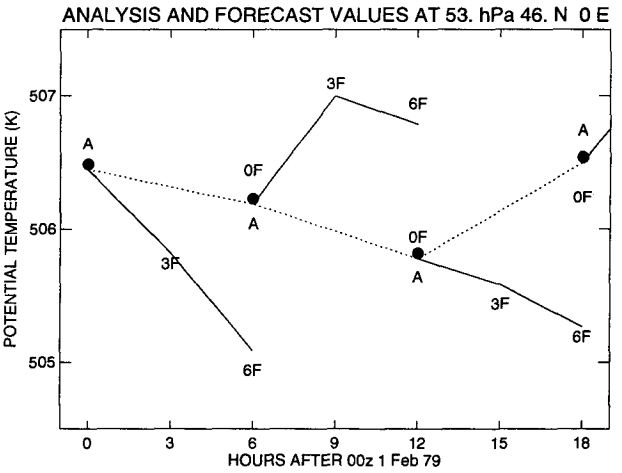

FIG. 3. Time series of potential temperature values taken from the assimilation process at 53 hPa 46°N, 0°E beginning at 0000 UTC 1 Feb 1979. Each solid curve is time series from a single GCM forecast. *A* is the analysis used as the initialization. The 3- and 6-hour forecasts are labeled 3F and 6F. Time series of successive analyses are shown by the dotted line.

The January mean value for each of the terms in (1) was calculated from the 0000 UTC forecast fields. The first term (mean vertical heat advection), the third term (horizontal eddy heat flux convergence), and the sum of all six terms (net balance), averaged from January 1979, are shown in Fig. 4a. The second (mean horizontal heat advection), fourth (vertical eddy heat flux convergence), fifth (potential temperature tendency), and sixth (diabatic heating rate) are not shown because they are all small compared to the mean vertical heat advection and the horizontal eddy heat flux convergence.

It is immediately apparent that the six terms in (1) are not balanced. Although it is not possible to ascertain which terms are in error, insight is gained by considering the relative magnitudes of the terms given here compared with other reported heat budgets. Using a GCM, Mahlman and Moxim (1978) report that tracer simulations in the stratosphere show that the mean vertical heat advection and the horizontal eddy flux convergence are the largest terms and are nearly balanced. Furthermore, when the nonacceleration theorem is satisfied, potential temperature should behave in a similar manner. O'Neill (1980) reports a near balance at 10 mb between the mean vertical heat advection term and the horizontal eddy heat flux convergence expected from quasigeostrophic theory. The residual of these two terms is dominated by the diabatic heating rate. Such behavior is not seen in Fig. 4a. In the Northern Hemisphere, the mean vertical and horizontal eddy flux convergence terms are the largest terms, but the expected near balance is not observed. The net balance term shown in Fig. 4a is in fact larger than $\bar{\theta}_t - \bar{Q}$ shown in Fig. 4b, and is sometimes nearly as large as the vertical heat advection term. The values of horizontal eddy heat flux convergence reported by Oort (1983) for this period are similar to those derived from the assimilation, which suggests that the magnitude of the vertical advection term from the assimilation is too large. In the Southern Hemisphere, where there are known analysis problems, there is not even a qualitative balance between the mean vertical advection term and the horizontal eddy heat flux convergence.

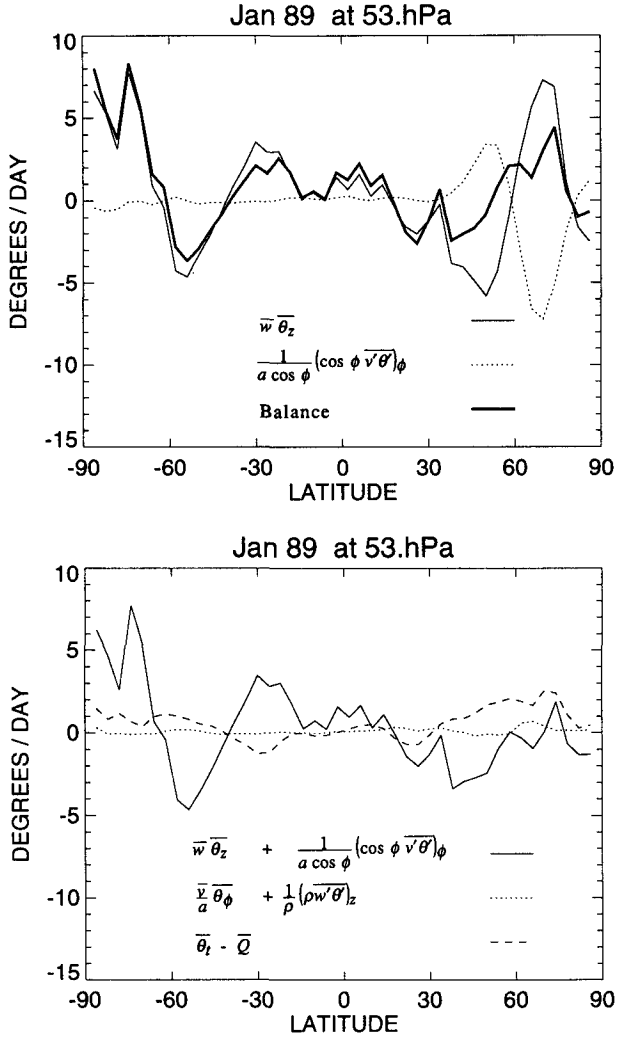

FIG. 4. (a) and (b) Selected terms from the zonal mean thermodynamic equation derived from assimilated data at 53 hPa January 1989.

The nonzero balance term in the heat budget affects the mean transport circulation of the model. The mean residual circulation is commonly employed to represent this mean mass transport in 2D models. To examine the problem further, we derive the residual circulation via two methods. These two representations of the residual circulation are related to each other through the thermodynamic equation. After dividing by the static stability $\bar{\theta}_z$, Eq. (1) may be rewritten

$$\bar{w} + \frac{1}{a\cos\phi}(\cos\phi\overline{v'\theta'})_\phi/\bar{\theta}_z \approx \frac{\bar{Q} - \bar{\theta}_t}{\bar{\theta}_z}.$$

The vertical eddy heat flux convergence and the mean horizontal heat advection are small compared to the other terms and have been neglected. The right- and left-hand side provide two expressions for the residual circulation, which we will denote as $\bar{w}_1^*$ and $\bar{w}_2^*$. On the left is the definition of $\bar{w}^*$ given by Andrews and McIntyre (1976),

$$\bar{w}_1^* = \bar{w} + \frac{1}{a\cos\phi}(\cos\phi\overline{v'\theta'})_\phi/\bar{\theta}_z.$$

On the right is the expression from Dunkerton (1978), who showed that the residual circulation could be derived from the potential temperature tendency and the mean diabatic heating rates according to

$$\bar{w}_2^* = \frac{\bar{Q} - \bar{\theta}_t}{\bar{\theta}_z}.$$

Figure 4b shows the combinations of terms required to calculate $\bar{w}_1^*$ (the mean vertical heat advection plus the horizontal eddy heat flux convergence) and $\bar{w}_2^*$ (the

potential temperature tendency minus the diabatic heating rate). It is clear that the values derived for $\bar{w}_1^*$ and $\bar{w}_2^*$ are quite different. The combination of mean horizontal heat advection and vertical eddy heat flux convergence is also shown on the figure; this sum is small compared to the other two combinations and does not influence the thermodynamic balance.

The difference between the two residual circulations is attributed to the potential temperature tendency. A tendency taken from a time series of successive 6-hour forecasts is used in $\bar{w}_2^*$. The instantaneous prognostic temperature tendency during the forecast at 6 hours is different from this. During the forecast, the wind fields and potential temperature satisfy the thermodynamic equation and it is these winds that are used to determine $\bar{w}_1^*$. Therefore, the instantaneous temperature tendency during the forecast at 6 hours is implicit in $\bar{w}_1^*$. The vertical wind field produced by the assimilation is most strongly influenced by the incorrect potential temperature tendency; the vertical wind responds to maintain balance in the model thermodynamic equation. Thus, the expected near balance between the vertical heat advection and the horizontal eddy heat flux convergence is not observed for the analysis fields.

If the assimilated winds were in the expected thermodynamic balance the residual circulations derived by these two methods would be almost identical. The monthly mean values at 50 mb are compared in Fig. 5. The circulation calculated from the definition $\bar{w}_1^*$ has larger upward motion in the tropics and downward motion in the middle latitudes compared with the circulation calculated from the thermodynamic balance using $\bar{w}_2^*$. The stronger circulation apparently produces excessively high column ozone values in the midlatitudes and excessively low column values in the tropics, consistent with the errors found in the simulation.

A 2D ozone simulation was performed using both a circulation derived from the definition $\bar{w}_1^*$ and a circulation derived from the heating rates using $\bar{w}_2^*$. Results are shown in Fig. 6. In both cases, the horizontal diffusion values are derived to be consistent with the wind fields (Newman et al. 1988). Although the horizontal diffusion values are different, they are not large enough to explain significant differences in the modeled constituent fields. The ozone calculated using the circulation derived from $\bar{w}_1^*$ deviates immediately from the initial condition. After only 11 days integration the ozone calculated in this way shows unrealistically high values in the midlatitudes accompanied by very low values in the tropics, as shown in Fig. 6. For this short integration, the ozone calculated using the circulation derived from thermodynamic balance using $\bar{w}_2^*$ remains close to the initial value for middle and tropical latitudes. TOMS measurements are in good agreement with the behavior of the ozone calculated using $\bar{w}_2^*$.

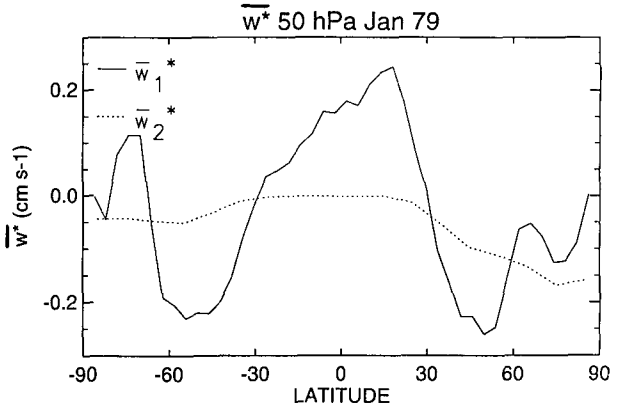

FIG. 5. Zonal mean residual vertical velocity calculated from $\bar{w}_1^*$ (solid) and calculated from $\bar{w}_2^*$ (broken) for January 1979 at 50 hPa.

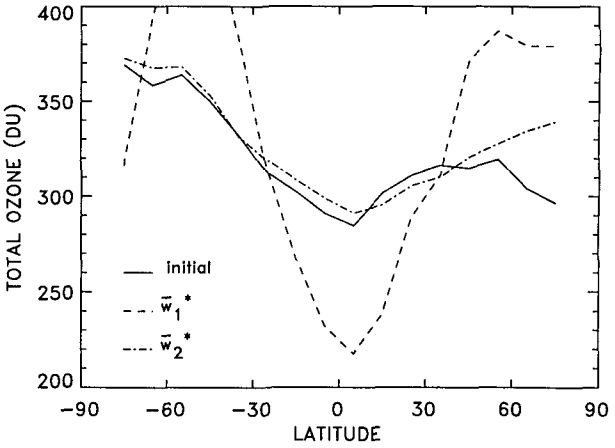

FIG. 6. Results of two 2D model runs with identical initialization and horizontal diffusion coefficients. Shown is zonal mean total column ozone in Dobson units at initialization (solid) and after 11 days of integration using residual circulation from $\bar{w}_1^*$ (broken) and from $\bar{w}_2^*$ (dashed–dotted).

5. Discussion

These 2D circulations were derived to help diagnose the cause of the differences between the 3D transport simulations and the satellite observations. The 2D ozone simulation driven by the circulation derived from the definition $\bar{w}_1^*$ is qualitatively similar to the 3D ozone simulation. This indicates that for the 3D transport model the mean meridional mass circulation that is actually responsible for the unrealistic buildup of gradients is more like the circulation calculated from the definition $\bar{w}_1^*$ than the circulation calculated from the heating rates using $\bar{w}_2^*$. This discrepancy is due to the near balance in the assimilated fields between the poorly determined potential temperature tendency and the mean vertical heat transport, which produces excessively large values of the vertical velocity. The close tracking of the net balance curve with the mean vertical term in Fig. 4a supports this contention. The horizontal eddy heat flux, which should balance the vertical term,

is not as disturbed by the imbalance and exhibits a qualitative similarity with the values given by Oort (1983).

Comparisons with constituent data show that the residual circulation $\bar{w}_2^*$, which is dominated by the diabatic heating rate, provides a better simulation. This demonstrates that the conceptual model of transport based on the transformed Eulerian mean formulation is valid (Andrews and McIntyre 1976; Edmon et al. 1980). There are many causes within the assimilation system for the unrealistic balance produced between the mean vertical heat advection and the temperature tendency. The assimilation system is always responding to the insertion of data. There are imbalances because of errors in the data, as well as due to inaccuracies in model numerics and parameterizations. These imbalances can excite unwanted gravity waves in the GCM, which may influence the temperature tendency in the GCM. These problems involving data insertion are inherent to assimilation procedures. Producing the proper thermodynamic balance is a core problem in the global mass transport, and that lack of the appropriate balance compromises the long term quality of the transport simulation.

The results suggest one form of postprocessing the data to force a physically realistic thermodynamic equilibrium in the system. The 2D experiments suggest that the transport derived from the diabatic information is close to reality. Therefore, it is possible to postprocess the 3D wind field iterating between the thermodynamic equation and the continuity equation, letting the diabatic heating provide the primary information to estimate the vertical velocity. Pilot calculations show promising impact on stratospheric transport calculations.

It is also possible to correct for the lack of thermodynamic equilibrium during the assimilation process. One approach, dynamic diabatic initialization (DDI) (Fox-Rabinovitz and Gross 1993), runs the model in order to obtain an estimate of the diabatic terms in the equation. The model is then initialized with fields that have some degree of both dynamical and diabatic balance with the forecast model. Initial experiments with DDI give a better representation of the tropics, and are at least qualitatively similar to the postprocessing procedure described above.

Acknowledgments. We thank Mark R. Schoeberl for constructive comments on this manuscript. The authors acknowledge NASA Headquarters High Speed Research Program for support.

REFERENCES

Allen, D. J., A. R. Douglass, and R. B. Rood, 1991: Application of a monotonic upstream transport scheme to three-dimensional constituent transport calculations. *Mon. Wea. Rev.*, **119,** 2456–2464.

Andrews, D. G., and M. E. McIntyre, 1976: Planetary waves in horizontal and vertical shear: The generalized Eliassen-Palm relation and the mean zonal acceleration. *J. Atmos. Sci.*, **33,** 2031–2048.

Baker, W. E., S. C. Bloom, J. S. Woolon, M. S. Nestler, E. Brin, T. W. Schlatter, and G. W. Brantstator, 1987: Experiments with a three-dimensional statistical objective analysis scheme using FGGE data. *Mon. Wea. Rev.*, **115,** 272–296.

Daley, R., 1991: *Atmospheric Data Analysis.* Cambridge University Press, 457 pp.

Douglass, A. R., C. H. Jackman, and R. S. Stolarski, 1989: Comparison of model results transporting the odd nitrogen family with results transporting odd nitrogen species. *J. Geophys. Res.*, **94,** 9862–9872.

Dunkerton, T., 1978: On the mean meridional mass motions of the stratosphere and mesosphere. *J. Atmos. Sci.*, **35,** 2325–2333.

Edmon, H. J. J., B. J. Hoskins, and M. E. McIntyre, 1980: Eliassen-Palm cross sections for the troposphere. *J. Atmos. Sci.*, **37,** 2600–2616.

Fox-Rabinovitz, M. S., and B. D. Gross, 1993: Diabatic dynamic initialization. *Mon. Wea. Rev.*, **121,** 549–564.

Geller, M. A., E. R. Nash, M. F. Wu, and J. E. Rosenfield, 1992: Residual circulation calculated from satellite data: Their relations to observed temperature and ozone distributions. *J. Atmos. Sci.*, **49,** 1127–1137.

Holton, J. R., 1986: Meridional distribution of stratospheric trace constituents. *J. Atmos. Sci.*, 1238–1242.

Mahlman, J. D., 1985: Mechanistic interpretation of stratospheric tracer transport. *Advances in Geophysics,* Vol. 28A, Academic Press, 301–323.

——, and W. J. Moxim, 1978: Tracer simulation using a global general circulation model: Results from a midlatitude instantaneous source experiment. *J. Atmos. Sci.*, **35,** 1340–1374.

Newman, P. A., M. R. Schoeberl, A. Plumb, and J. E. Rosenfield, 1988: Mixing rates calculated from potential vorticity. *J. Geophys. Res.*, **93,** 5221–5240.

O'Neill, A., 1980: Dynamical processes in the stratosphere: Wave motion. NATO Advanced Study Institute on Atmospheric Ozone, FAA-EE-80-20 (NTIS). Springfield, VA.

Oort, A. H., 1983: Global atmospheric circulation statistics, 1958–1973 NOAA Prof. Paper No. 14. U.S. Department of Commerce, Washington D.C. 20230.

Prather, M. J., 1986: Numerical advection by conservation of second-order moments. *J. Geophys. Res.*, **91,** 6671–6681.

Rood, R. B., D. J. Allen, W. E. Baker, D. J. Lamich, and J. A. Kaye, 1989: The use of assimilated stratospheric data in constituent transport calculations. *J. Atmos. Sci.*, **46,** 687–701.

——, A. R. Douglass, J. A. Kaye, M. A. Geller, C. Yuechen, D. J. Allen, E. M. Larson, E. R. Nash, and J. E. Nielsen, 1991: Three-dimensional simulations of wintertime ozone variability in the lower stratosphere. *J. Geophys. Res.*, **96,** 5055–5071.

——, J. E. Nielsen, R. S. Stolarski, A. R. Douglass, J. A. Kaye, and D. J. Allen, 1992: Episodic total ozone minima associated effects on heterogeneous chemistry and lower stratospheric transport. *J. Geophys. Res.*, in press.

Rosenfield, J. E., M. R. Schoeberl, and M. A. Geller, 1987: A computation of the stratospheric diabatic circulation using an accurate radiative transfer model. *J. Atmos. Sci.*, **44,** 859–876.

Takano, K., W. E. Baker, E. Kalnay, D. J. Lamich, J. E. Rosenfield, and M. A. Geller, 1987: Forecast Experiments with the NASA/GLA stratospheric/tropospheric data assimilation system. *J. Meteor. Soc. Japan,* **67,** 83–89.

van Leer, B., 1974: Towards the ultimate conservative difference scheme, II, monotonicity and conservation combined in a second order scheme. *J. Comput. Phys.*, **14,** 361–370.

World Meterorological Organization (WMO), 1986: Atmospheric Ozone: 1985. WMO Rep. 16, Washington D.C., 478 pp.